analytical chemistry

Article

pubs.acs.org/ac

Enhancing Ion Yields in Time-of-Flight-Secondary Ion Mass Spectrometry: A Comparative Study of Argon and Water Cluster Primary Beams

Sadia Sheraz née Rabbani,[†,‡] Irma Berrueta Razo,[†,§] Taylor Kohn,[†,‡] Nicholas P. Lockyer,[†,§] and John C. Vickerman*[,†,‡]

[†]Manchester Institute of Biotechnology, The University of Manchester, Manchester, U.K.

[‡]School of Chemical Engineering and Analytical Science, The University of Manchester, Manchester, U.K.

[§]School of Chemistry, The University of Manchester, Manchester, U.K.

Supporting Information

ABSTRACT: Following from our previous Letter on this topic, this Article reports a detailed study of time-of-flight-secondary ion mass spectrometry (TOF-SIMS) positive ion spectra generated from a set of model biocompounds (arginine, trehalose, DPPC, and angiotensin II) by water cluster primary ion beams in comparison to argon cluster beams over a range of cluster sizes and energies. Sputter yield studies using argon and water beams on arginine and Irganox 1010 have confirmed that the sputter yields using water cluster beams lie on the same universal sputtering curve derived by Seah for argon cluster beams. Thus, increased ion yield using water cluster beams must arise from increased ionization. The spectra and positive ion signals observed using cluster beams in the size range from 1 000 to 10 000 and the energy range 5−20 keV are reported. It is confirmed that water cluster beams enhance proton related ionization over against argon beams to a significant degree such that enhanced detection sensitivities from 1 μm^2 in the region of 100 to 1 000 times relative to static SIMS analysis with Ar_{2000} cluster beams appear to be accessible. These new studies show that there is an unexpected complexity in the ionization enhancement phenomenon. Whereas optimum ion yields under argon cluster bombardment occur in the region of $E/n \geq 10$ eV (where E is the beam energy and n the number of argon atoms in the cluster) and fall rapidly when $E/n < 10$ eV; for water cluster beams, ion yields increase significantly in this E/n regime (where n is the number of water molecules in the cluster) and peak for 20 keV beams at a cluster size of 7 000 or $E/n \sim 3$ eV. This important result is explored further using D_2O cluster beams that confirm that in this low E/n regime protonation does originate to a large extent from the water molecules. The results, encouraging in themselves, suggest that for both argon and water cluster beams, higher energy beams, e.g., 40 and 80 keV, would enable larger cluster sizes to be exploited with significant benefit for ion yield and hence analytical capability.

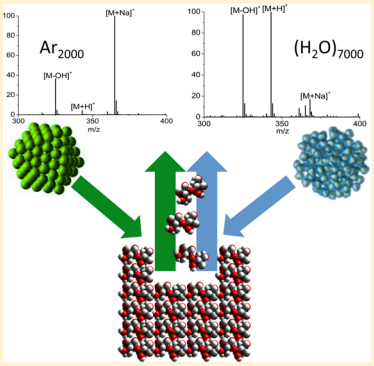

It is now widely accepted that time-of-flight-secondary ion mass spectrometry (TOF-SIMS) has great potential as one of a number of mass spectrometric techniques for 2D and 3D imaging of the distribution of molecular chemistry in organic and biological systems.[1−4] While it is limited to molecules of mass below about 2000 Da, compared to matrix-assisted laser desorption ionization (MALDI), desorption electrospray ionization (DESI), and related techniques, it has higher spatial resolution capabilities that offer the promise of submicrometer, and hence use in biology subcellular analysis.[5] However, as is common with all desorption mass spectrometries, ion yields are very low. Ionization probabilities below 10^{-5} are very common.[6] As a result, the molecular ion useful yields from a 1 μm^2 pixel area are less than 0.01 under *static* conditions (<1% of surface removed to minimize ion beam induced chemical damage). The advent of C_{60} and more recently argon cluster ions beams has lifted the static restriction on TOF-SIMS, but even under these more advantageous conditions, signal levels from 1 μm^2 are at most only a few ions, certainly too few to make submicrometer imaging a useful technique. There is therefore a very strong impetus to find ways of raising the ion yield.

Although it is possible to enhance the secondary ion yields from organic and bio-organic analytes by adding compounds or metals to the surface,[7−12] these methods are usually system specific, and the addition of further chemistry to what are frequently quite complex materials is not always to be recommended. Additionally they are not readily applicable in 3D analytical applications.

Ideally it would be preferable to enhance ion yield via developments in primary ion beam technology. There have been a number of these over the last 20 years. The use of gold and bismuth cluster beams based on liquid metal technology enhanced yields of ions around m/z 300−800 although still

Received: November 17, 2014
Accepted: January 14, 2015
Published: January 14, 2015

DOI: 10.1021/ac504191m
Anal. Chem. 2015, 87, 2367−2374

constrained by the static limit because of the ion beam damage resulting from their use.[13,14] SF_5 and C_{60} beams enhanced the relative yield of high mass ions by factors up to 1000 compared to atomic primary beams, and because the static limit could be lifted in many cases much more of the analyte could be used for analysis, providing a further improvement in detection sensitivity.[15,16] Most recently argon cluster ion beams have provided a further significant development in low damage primary ion beam technology.[17] They have been employed in dual beam analysis as low damage sputter beams, but Matsuo's first studies advocated the use of these beams for analysis.[18] A number of studies have demonstrated that the larger cluster sizes Ar_{2000} to Ar_{4000} increase the yield of molecular species with little bombardment-induced damage. Studies in this laboratory have shown that 20 keV argon cluster beams can deliver spectra of quality from molecules such as angiotensin,[19] and the amino acid sequence of the peptide could be probed.[20] Many other studies on biomolecules have shown similar capability.[21−26] Recently Angerer et al. have demonstrated that a 40 keV Ar_{4000} beam is very effective in generating good yields of lipid and glycoside ions from tissue samples.[27] It is clear that the enhanced energy and larger cluster size is beneficial in increasing the yield of the molecular species with minimal bombardment-induced damage.

The capability of large cluster beams in delivering higher yields of larger fragments and "molecular" ions in spectral analysis has engaged the interest of the theorists. Seah et al. have recently described an empirical set of equations to describe the observation that as E/n (beam energy divided by the number of atoms in the cluster) declines, the prevalence of smaller sputtered fragment ions falls relative to the yield of large fragments or molecular ions.[28] This is a consequence of the lower average binding energy to the sample of the larger fragments and molecules per unit mass, which is reflected in the equation by the parameter A_m. The role of such a parameter is also implied from molecular dynamics (MD) simulations of sputtering by large clusters.[29] In simulations of argon cluster sputtering, Postawa and Garrison have shown that there is a transition around $E/n \sim 10$ eV below which the cluster seems to act as whole and sputtering is almost by a "washing" mechanism, sweeping larger species from the surface.[30,31] Thus, the cluster as a whole penetrates further into the analyte, and emission of larger secondary clusters occurs from a low energy region around the periphery of the impact site. There is however a potential downside to this conclusion. As shown in Figure 11 in Seah's paper, if E/n is lowered too much, the ion yield falls, probably because the impact energy of the cluster is less and less efficient in ionizing the molecules.[28] It seems that although argon cluster beams can be tuned to optimize higher mass sputter yield, there is still a need for additional methods to increase the ion yield.

An approach that has shown some success in enhancing ionization is based on the observation that the presence of water, either adventitious or intentionally added, enhances the yield of $[M + H]^+$ ions.[32−37] On the basis of these observations and the ideas inherent in proton reaction mass spectrometry, our first comparative study of ion yields from a set of biorelated compounds using 10 keV Ar_{1000}^+ and 10 keV $(H_2O)_{1000}^+$ cluster ions showed that a 10 times or more increase in $[M + H]^+$ and related ion signals resulted from the use of the water cluster beam compared to the argon cluster beams.[38] The bombardment-induced molecular damage was minimal, and consequently the ion yields could be accumulated offering the promise of a more useful signal from the 1 μm^2 target. Other researchers have been exploring the use of an electrospray beam.[39] This would certainly deliver a very dense region of water-related species. However, handling, controlling, and focusing an electrospray beam in a vacuum is challenging and indeed the density of water might be too great.[40] With a similar aim of increasing ion yield, there has been a very recent study of use of ionic liquids to form a primary beam for SIMS in an electrospray arrangement. However, the downside is the deposition of the compound on the analyte.[41]

The mechanism of enhancement by water cluster beams is a matter of speculation at this stage, but since water cluster ions will primarily be bound together by hydrogen bonds, the cluster will be relatively strongly held together. Hydrogen bonding energy of a $(H_2O)_{20}$ cluster is estimated to be around 8.5 eV,[42] and the bond energy of the HO−H bond in water is about 5 eV, so it is likely that at low E/n the large cluster ion will remain relatively intact on impact and the water molecule itself may behave more as a single entity than falling apart. The aim of this research is to explore further the behavior of water clusters in delivering higher ion yields relative to comparable argon clusters.

EXPERIMENTAL SECTION

Material and Sample Preparation. Ion yield studies were carried out on thin spin-cast films of four biorelated compounds: arginine, trehalose, dipalmitoylphosphatidylcholine (DPPC), and angiotensin II. The preparation of the films is outlined in the Supporting Information.

TOF-SIMS Studies. TOF-SIMS analysis was performed on a J105 3D Chemical Imager (Ionoptika Ltd. U.K.) described in detail previously.[43,44] The J105 is equipped with a 40 keV C_{60}^+ primary ion beam (Ionoptika Ltd., U.K.). A 20 keV gas cluster ion beam (GCIB) system also supplied by Ionoptika Ltd. and described elsewhere[19] forms the basis of a second primary beam system that can provide either argon cluster or water cluster beams, the details of which are provided in the Supporting Information.

Sputtering Studies. To investigate the sputter yields of water cluster beams relative to C_{60} and argon cluster beams, we have focused most of our study on Irganox 1010 that has been thoroughly characterized by the U.K. National Physical Laboratory.[45−47] We have used spin-cast films made in house and thermally evaporated films obtained from NPL. The protocols for film preparation and sputter yield measurement are presented in detail in the Supporting Information.

Ion Signal Studies. This research is focused on enhancing the ion yield. The signal detectable that reflects the ion yield will be partly determined by instrumental factors such as transmission and the mode of operation of the detector system. Unlike many TOF-SIMS systems, but like most other mass spectrometers, we are using an analogue detector/measurement system such that each ion impact on the detector is amplified and the output signal may be higher than with a conventional single ion counting SIMS system. In this Article, it is the detected secondary ion signal intensity that is reported.

Positive ion spectra after a primary ion dose of 5×10^{11} ions cm^{-2} followed by a dose dependent study of spectral changes up to a dose of 1 to 3×10^{13} ions cm^{-2} were obtained from the four biorelated samples using 20 keV argon cluster beams Ar_{1000} to Ar_{6000} and 20 keV water cluster beams $(H_2O)_{1000}$ to $(H_2O)_{10000}$. Some studies of the variation of ion signal as a function of beam energy (5, 10, and 20 keV) at a given cluster

DOI: 10.1021/ac504191m
Anal. Chem. 2015, 87, 2367−2374

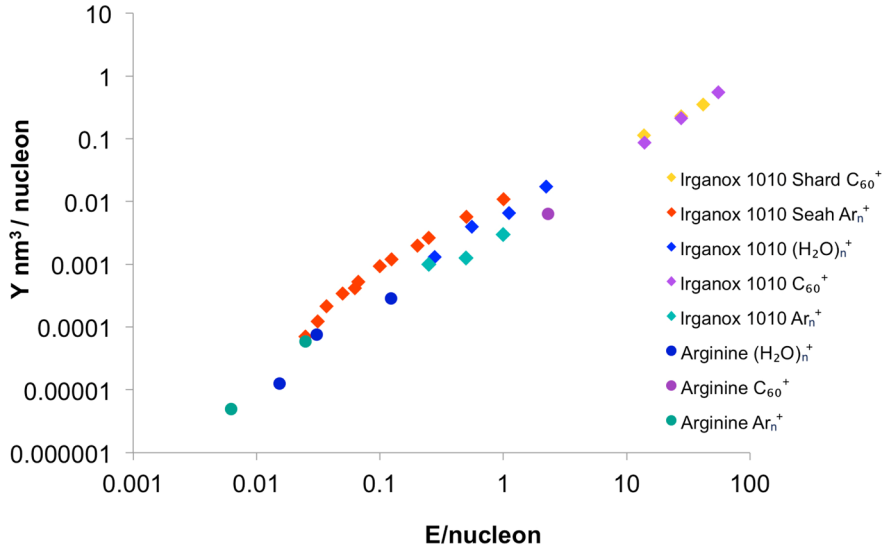

Figure 1. Sputter yields (Y) from Irganox 1010 and arginine films using C_{60}, argon, and water cluster beams from this work compared to data reported by Seah[49] and Shard et al.[48] using C_{60} and argon cluster beams plotted as Y in nm^3/nucleon as a function of E/nucleon.

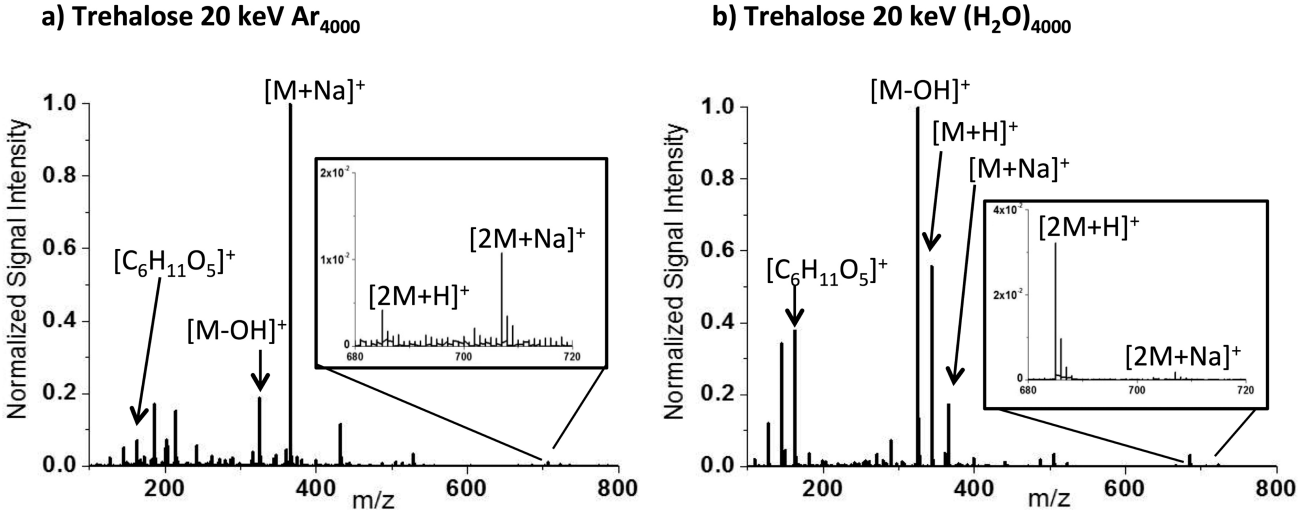

Figure 2. Spectra from trehalose obtained using (a) 20 keV Ar_{4000} and (b) 20 keV $(H_2O)_{4000}$ cluster beams with a primary ion dose of 5×10^{11} ions cm^{-2}. The spectra are referenced to the base peak for each analysis.

size were also carried out over the same ion dose range. In order to correct for any instrumental variations and to confidently compare ion yields between experiments using the different cluster beams, all ion signals were referenced to the total ion signal observed for each compound from a 20 keV C_{60} analysis after a dose of 3×10^{13} ions cm^{-2}. The reference experiment was carried out before each series of argon or water cluster beam experiments.

RESULTS AND DISCUSSION

Sputter Yield Studies. The purpose of these measurements is to check that the increased ion signals observed in our first study and in this study were not primarily due to higher sputter yields under water beams. To validate the methods used to determine the sputter yields, we first obtained measurements on Irganox 1010 using 10, 20, and 40 keV C_{60} and compared the results with those obtained by Shard et al.[48] In Figure 1, the sputter yields of 20 keV Ar_{500} and Ar_{2000} are compared to those from 10 keV $(H_2O)_{500}$ and $(H_2O)_{2000}$ and 20 keV $(H_2O)_{500}$, $(H_2O)_{2000}$, and $(H_2O)_{4000}$. The figure places the data in the format of the so-called "universal sputtering curve" due to Seah.[49] Because sputter yields from three different primary beams are being compared, the data is plotted as Y in nm^3/nucleon against the beam energy E/nucleon, where E is the cluster beam energy. The argon cluster yield data for Irganox 1010 presented in Seah's paper is included on the plot. We have also included the C_{60} data to show how it all integrates together rather closely. The only significant deviation is that the argon cluster yields measured in this work are somewhat lower than those recorded on the Seah curve. We are not sure why this should be; however, the water cluster yields sit very close to Seah's argon curve.

To provide a connection with the biological samples in this study, sputter yields from films of arginine were also monitored. This data also included in Figure 1 and fits nicely on the curve too. The overall conclusion is that the sputter yields for water cluster beams are not significantly different from other cluster beams of similar cluster size. The Seah universal equation is empirical and suggests that the only significant parameter is E/n. Postawa et al. have recently suggested that including the

DOI: 10.1021/ac504191m
Anal. Chem. 2015, 87, 2367−2374

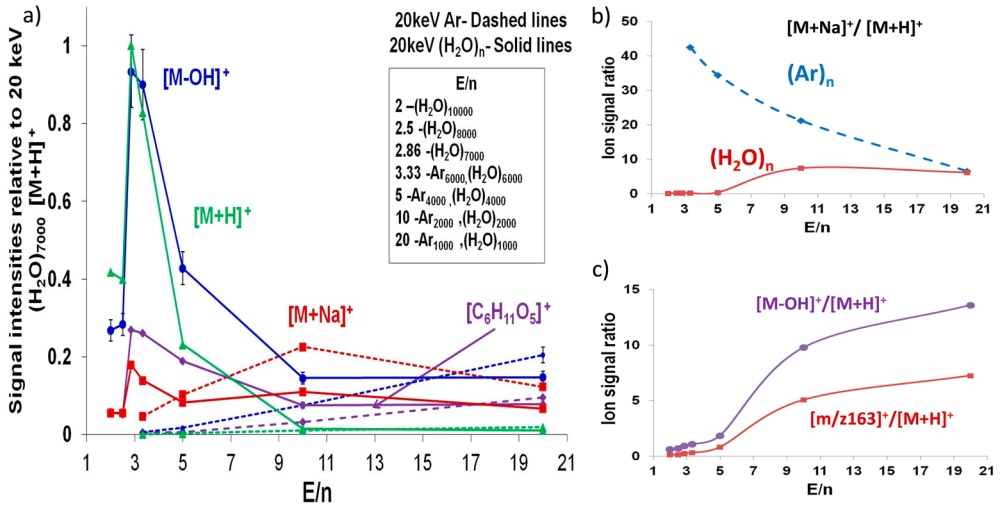

Figure 3. (a) Plot of relative trehalose ion signals (normalized to the maximum ion signal of $[M + H]^+$) after an ion dose of 5×10^{11} ions cm^{-2} as a function of E/n for the 20 keV argon and water cluster beams used. $[M + H]^+$ variation denoted by green lines (dashed for argon beams, continuous for water); $[M - OH]^+$ denoted by blue lines; $[M + Na]^+$ denoted by red lines; and $[C_6H_{11}O_5]^+$, m/z 163, by purple lines. For the sake of figure clarity, error bars reflecting the detected signal variation of multiple measurements are provided only for the $[M - OH]^+$ ion for the water and argon. The data uncertainty is the same for all the ions. (b) The variation of the $[M + Na]^+/[M + H]^+$ signal ratio from trehalose as a function of E/n for Ar_n (dashed blue line) and $(H_2O)_n$ cluster primary beams (continuous red line). (c) Ratio of $[M - OH]^+$ and the m/z 163 fragments to $[M + H]^+$ ion signals for trehalose as a function of E/n for water beams after an ion dose of 5×10^{11} ions cm^{-2}. Purple line $[M - OH]^+/[M + H]^+$, red line m/z $163/[M + H]^+$.

binding energy of the analyte into the formalism would provide a more physical understanding of the process and contribute to making the equation more "universal".[50] For our purposes, the plot in Figure 1 draws together the relevant data to show the close alignment of argon, C_{60}, and water sputtering. It is interesting that it seems that the water molecule can be regarded as a sputtering unit on par with the argon atom.

Ion Yields from Water Cluster Beams Relative to Argon Cluster Beams. The positive ion spectra from four representative compounds have been studied, i.e., arginine, trehalose, angiotensin II, and DPPC. The spectra obtained using a 20 keV Ar_{4000} and 20 keV $(H_2O)_{4000}^+$ ion beam are presented in Figure 2 for trehalose and Figure S1 in the Supporting Information for the other compounds for an ion dose of 5×10^{11} ions cm^{-2}. Although the spectra arising from argon and water cluster beams are qualitatively similar, there are some notable differences. Where sodium is present, the $[M + Na]^+$ ion signals are significantly stronger in the argon spectra, and $[M + H]^+$ and related peaks are more evident in water cluster spectra.

Figure S2 in the Supporting Information shows how the ion signals relative to the total ion signal from trehalose vary as a function of ion dose for Ar_{2000} and Ar_{4000} compared to $(H_2O)_{2000}$ and $(H_2O)_{4000}$ beams. The ion signals do not decay significantly over the dose range up to 3×10^{13} ion cm^{-2}. Under argon cluster bombardment it is the $[M + Na]^+$ ion that predominates, increasing over a dose of about 5×10^{12} ions cm^{-2} before reaching something of a plateau. The ions that rely on proton addition are less than 20% of the $[M + Na]^+$ intensity. The $[M-OH]^+$ ion that results from the loss of water from the protonated $[M + H]^+$ ion is the most intense, while the monosaccharide fragment ion $[C_6H_{11}O_5]^+$ is very weak. Under 20 keV $(H_2O)_{4000}$ cluster bombardment, the order of ion yield is almost completely reversed. The ions associated with proton addition predominate with the $[M-OH]^+$ ion the most intense, and the $[M + Na]^+$ ion yield is less than 20% of the $[M + H]^+$ yield. With the 20 keV $(H_2O)_{2000}$ beam at low dose, the $[M-OH]^+$ ion is also the most intense, but as the primary ion dose increases the $[M + Na]^+$ yield overtakes it. Although the $[M + H]^+$ yield is somewhat greater than under argon cluster beams, the relative order of ion yields is the same as with argon. This data suggests that with a large water cluster the ionization by protonation is favored, but the smaller water cluster such that E/n = 10 eV displays behavior very similar to the argon cluster beams. The other compounds studied show very similar behavior. The larger the cluster the smaller the decay in signal intensity to the steady state; the argon clusters favor sodiated adducts where these are possible and the larger water clusters where $E/n \leq 10$ eV favor proton related secondary ions.

To compare the ion yields obtained using the argon and water beams, we plot the variation of the ion signals for the principal ions assigned in Figure 2 spectra against E/n for the 20 keV cluster beams where n varies from 1 000 to 10 000.

Figure 3a shows a set of such plots for trehalose following an ion dose of 5×10^{11} ions cm^{-2} and Figure S3 in the Supporting Information at steady state after an ion dose of 3×10^{13} ions cm^{-2}. Comparing the plots from the argon beams with the water beams for the disaccharide pseudomolecular ion $[M + H]^+$ at m/z 343 and the related $[M - OH]^+$ ion at m/z 325 we immediately see sharply contrasting behavior. Whereas the yields fall from Ar_{2000} to close to zero at Ar_{6000} (E/n 10–3.3 eV), the water beam $[M + H]^+$ and $[M - OH]^+$ signals rise sharply from about the same level as Ar_{2000} using $(H_2O)_{2000}$ to 80 and ~13 times the Ar_{2000} signal, respectively, using 20 keV $(H_2O)_{7000}$. Enhanced proton attachment is clearly favored below E/n = 10 eV, maximizing at about 3 eV. This differing behavior of the argon and water cluster beams is seen to varying degrees for all the compounds in this study, see the Supporting Information, Figures S3–S6.

Although sodiation is not the focus of this paper, because many biosystems contain salt and sodiation represents an alternative ionization mechanism to protonation, the contrasting behavior of the $[M + Na]^+$ ion is worth a comment. A plot

DOI: 10.1021/ac504191m
Anal. Chem. 2015, 87, 2367–2374

of $[M + Na]^+/[M + H]^+$ as a function of E/n in Figure 3b underlines the fact that $[M + Na]^+$ is increasingly favored, mainly because the $[M + H]^+$ yield falls more rapidly. In contrast as the water cluster size increases, the $[M + Na]^+/[M + H]^+$ falls to a very low level because the $[M + H]^+$ yield rises rapidly.

Fragment Ion Yield. The yield of fragment ions also varies with cluster size. There are two sorts of fragments generated in SIMS. There are damage fragments having no real structural significance that result from the high-energy emission zone. The yield of such ions would be expected to fall as E/n falls as suggested by Seah.[28] However, there are other structurally related ions that are a result of metastable decay of parent or molecular ions whose yield will depend on the degree of excitation and stability of the emitted parent ion. The two structurally significant fragment ions particularly evident in the trehalose spectra are the $[M - OH]^+$ and $[C_6H_{11}O_5]^+$ ions. The ratio of these two ions to $[M + H]^+$ varies little under argon bombardment, whereas with the water beams, as shown in Figure 3c, the ratio falls sharply from around 14 and 7, respectively, with $(H_2O)_{1000}$ to less than 1 with $(H_2O)_{7000}$ indicating a sharp fall in this type of fragmentation as E/n falls below 10 eV, such that increased ionization is matched by decreased fragmentation. It is possible that the ionization process leaves the resulting $[M + H]^+$ ion in a lower energy state resulting in less metastable fragmentation. Similar effects are evident for the fragments of the other molecules studied.

Role of Cluster Size. From the above data, E/n delineates an energy regime for optimum molecular and fragment yield using argon and water cluster beams, for argon it is around 10 eV whereas for water the 2.5 eV < E/n < 5 eV regime seems to deliver the best $[M + H]^+$ and related ion yields. An important question for both analytical practice and in terms of understanding the mechanism of cluster beam ion generation is whether ion yield can be increased by increasing the cluster size at the optimum E/n. The study by Angerer et al. suggests that doubling the cluster size from 2000 to 4000 at E/n = 10 eV doubles the secondary ion yield.[27] The 40 keV beam energy cannot be accessed in this work, but we have observed the same result for argon clusters E/n = 5 eV. In other words, doubling the number of atoms in the argon cluster where the total beam energy increases to maintain a constant E/n delivers about twice the yield.

The effect of increasing the water beam cluster size at $E/n \sim$ 3 eV on the signal levels of the $[M + H]$ and $[M - OH]$ ions of trehalose has been monitored using 10 keV $(H_2O)_{3300}$, 15 keV $(H_2O)_{5000}$, and 20 keV $(H_2O)_{7000}$ beams. Figure S7 in the Supporting Information shows that doubling the cluster size doubles the ion signal. For these samples it is clear that large clusters are a "good thing" for ionization, and the optimum E/n for water beam ion yield enhancement is probably close to 3 eV. Increasing the *total* beam energy allows the use of larger clusters within the optimum E/n regime resulting in higher secondary ion yield.

Mechanism: A D_2O Cluster Ion Study. To try to clarify the mechanism of secondary ion generation in the two E/n regimes, the effect of using D_2O cluster beams instead of H_2O clusters in trehalose and DPPC analysis has been investigated. These two molecules are rather different. Trehalose is a disaccharide with four exchangeable hydrogens per sugar ring, three on the ring OH groups and one CH_2OH group. Proton ionization must occur at one of these OH groups. On the other hand DPPC has no exchangeable hydrogens. These two molecules were exposed to 20 keV D_2O cluster beams composed of 1000, 2000, and 4000 molecules, and the resulting spectra were compared to those obtained from similar argon and water cluster beams. Ion yield enhancement under D_2O cluster beams was very close to that observed for H_2O cluster beams of the same size. To ensure that any observed deuteration was due entirely to the D_2O cluster ion beam and not due to gas phase exposure to D_2O, both samples were exposed to the neutral $(D_2O)_{4000}$ cluster beam (i.e., the gas phase cluster beam emitted without ionization) for the time equivalent of an ion beam experiment and checked for any deuteration by C_{60} ion beam analysis. Under these conditions there was no evidence of deuterated secondary ions.

After $(D_2O)_n$ cluster ion beam exposure, the spectral behavior of the two compounds was rather different. In the case of DPPC two ions are influenced by the presence of deuterium: The $[M + H]^+$ ion at m/z 734.5 ($C_{40}H_{80}NO_8P$ + H) with its associated ^{13}C isotope component at m/z 735.5 of 44% relative intensity. This ion is formed by protonation of the negative phosphate on the choline headgroup leaving the positive charge on the quaternary nitrogen. The phosphocholine ion $(C_5H_{15}NPO_4)^+$ at m/z 184 with its m/z 185 ^{13}C component with 7% intensity is a little unusual. Two hydrogens are required for its formation.[51,52] SIMS with laser postionization suggests that a neutral phosphocholine fragment dissociates from the DPPC molecule via an intramolecular hydrogen transfer.[52]This neutral is then protonated from its environment, again at the phosphate group to form the m/z 184 ion. Figure 4 summarizes the deuteration results. The first

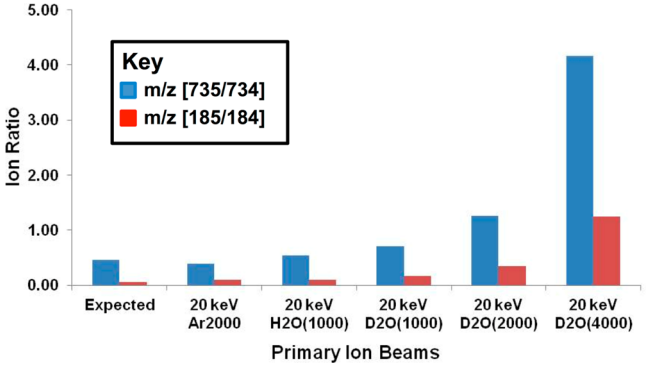

Figure 4. Ion signal ratios for m/z (735/734) and m/z (185/184) (the "expected" ratios are those which would arise from the ^{13}C contribution) from DPPC obtained with $(H_2O)_n$ and $(D_2O)_n$ cluster primary ion beams at a dose of 5×10^{11} ions cm^{-2}.

pair of columns show the expected ion ratios of m/z 735/734 and m/z 185/184, a consequence of the natural abundance of ^{13}C, 0.44 and 0.07, respectively. It can be seen that the yields from argon and water beams deviate little from this expected value. The 20 keV $(D_2O)_{1000}$ lifts the relative ion yields to a small degree, but almost within experimental error, a result which supports the observation earlier that above E/n = 10 eV argon and water cluster beams behave similarly. The $(D_2O)_{2000}$ beam results in a doubling of the m/z 735 to more than matching the yield of the m/z 734 peak (a ratio >1) reflecting the formation of a $[M + D]^+$ ion. The $(D_2O)_{4000}$ beam results in a m/z 735.5 peak intensity that is 4 times that of 734.5 suggesting very extensive deuteration in place of protonation. In parallel with these changes, in the m/z 184 peak region $(D_2O)_{2000}$ resulted in a doubling of the m/z 185 peak

DOI: 10.1021/ac504191m
Anal. Chem. 2015, 87, 2367−2374

suggesting some deuteration, the $(D_2O)_{4000}$ beam resulted in m/z 185 matching the yield of 184. These results confirm that the large water clusters, where E/n < 10 eV do contribute to ionization by proton attachment from cluster water molecules. As would be expected there is no deuterium attachment to the $[M + Na]^+$ ions.

The trehalose secondary ions behave rather differently. As with DPPC there was little effect on the spectra compared to argon and water beams using 20 keV $(D_2O)_{1000}$. However, under 20 keV $(D_2O)_{2000}$ and $(D_2O)_{4000}$ beams, all the secondary ions reliant on protonation: $[M + H]^+$, m/z 343, $[M - OH]^+$, m/z 325, the single sugar fragment, m/z 163 showed the development of several new peaks at m/z +1, +2, +3 and +4 as shown in Figure S8 in the Supporting Information. In line with our data so far, it is the 10 keV $(D_2O)_{4000}$ (E/n = 2.5 eV) beam that delivers the highest yields. Analyzing the $[M + H]^+$ and $[M + D]^+$ yields requires that the observed signals be corrected for the contributions due to ^{13}C that introduce additional peaks at, for example, m/z 344 (14%) and m/z 345 (3%). From the series of peaks between m/z 343 and 348 generated by 10 keV $(D_2O)_{4000}$, it is possible to conclude that relative to the $[M + H]^+$ yield about 25% $[M + D]^+$ is produced and about 16% of $[M - H + 2D]^+$, i.e., in addition to deuteration, one hydrogen has been exchanged. There are lower levels of exchange observed up to 4 ring hydrogens. Two comments can be made. First, in contrast to the DPPC result, it is significant that despite the large D_2O cluster size there is still significant protonation by hydrogen, about 50% with 10 keV $(D_2O)_{4000}$ judging from the relative yield to 10 keV $(H_2O)_{4000}$ for the m/z 343 ion. We are confident that while some small exchange with water in the vacuum system may occur, the great majority of the beam is D_2O, so we must conclude that significant activation of hydrogen arises from the beam impact on the sample. The fact that there is the possibility of a good deal of hydrogen exchange in trehalose will decrease the degree of deuteration relative to protonation by a significant extent. The kinetic isotope effect may also be involved and the rate of deuteration could be many times slower than protonation so competition in the reaction/emission zone could be significant. The second comment relates to the quite significant degree of hydrogen−deuterium exchange. It is clear that the larger the $(D_2O)_n$ cluster the greater the exchange effect. The fact that exchange is so large implies an intimate interaction between the $(D_2O)_n$ cluster and the sputtered molecules suggesting a mechanism based on a concerted process in the emission zone that accounts for a significant degree of protonation. A further pointer to an intimate association of trehalose and the water clusters in the emission zone is the appearance of peaks in the range m/z 362 to 364 and 381 to 385 that can be assigned to various combinations of ($M + H^+$ or $D^+ + H_2O$ or D_2O and $M + H^+$ or $D^+ + 2D_2O$). Similar complexes were shown to contribute to the formation of protonated trehalose in FABMS with glycerol.[53]

In summary, the data reported here from trehalose and the other compounds indicates that the energy per cluster beam component (E/n) is crucial for both cluster beam systems. This study and previous work shows that ion yield from argon cluster beams appears to maximize or plateau in the region of E/n = 10 eV and the larger the cluster size the higher the yield, so there are clear benefits in using higher energy beams. This work also shows that for $E/n \geq 10$ eV, the ion yields from water cluster beams are similar to those from argon beams. The chemistry of the beam in this E/n regime does not seem to be very important. The water cluster beams must possess too much energy for the water molecules to have time to interact significantly with the analyte molecules chemically, consequently they just seem to act as high-energy sputtering initiating particles. The absence of significant additional deuteration suggests that either the $[M + H]^+$ ions are MALDI type "Lucky Survivor" ions[54] formed during the sample preparation, or they are formed in the emission region by interaction with protons mainly arising from sputtering the analyte. The absence of a MALDI matrix to help form Lucky Survivor $[M + H]^+$ ions and separate them from neutralizing counterions would argue against that mechanism, although the higher yield of $[M + Na]^+$ ions particularly observed with argon cluster beams might arise through this route. A systematic study varying the salt content of the samples would be required to clarify this issue. However, MD studies have shown that preformed protonated ions can be expected to be emitted from the low energy periphery of a high energy primary ion impact site.[55,56] It is envisaged that some protons formed during high-energy fragmentation during the initial impact flow out to the periphery and encounter intact molecules. Protonated molecular ions are formed and emitted, possibly during a subsequent primary impact. The high energy required to form the protons by this mechanism would be consistent the behavior observed in the $E/n \geq 10$ eV region. As E/n falls below 10 eV, the $[M + H]^+$ yield falls rapidly with argon beams, presumably because there is insufficient energy for proton formation.

For the water cluster beams, however, the really interesting energy regime is E/n < 10 eV. The $[M + H]^+$ and related ion yields for all the compounds studied *increase* significantly with cluster size, reaching a maximum in the region of $E/n \sim 3$ eV. This intriguing result implies that the protonation process is a relatively low energy process. As outlined in the introduction, theory suggests that at these energies the clusters will maintain some sort of coherent action, perhaps even retaining their cluster geometry.[29−31] This may result in a crater of cluster dimensions and mixing of the cluster components with the analyte, perhaps even generating something akin to a hydrated environment for the sputtered analyte species. The deuteration results would support such a concept. Thus, on impact a concerted process may be involved in the emission zone. Presumably in order for water to facilitate ionization via proton transfer, there has to be enough energy to activate such transfer via molecular dissociation or activate reaction with the energized departing molecules and fragments; hence, there is an optimum E/n for enhanced protonation.

Ion Detection per 1 μm^2. Finally does this work advance the stated aim to increase ion yields in order to increase the feasibility of submicron analysis and imaging in biological research? Figure 5 reports the ion signal levels detected per 1 μm^2 from a 5×10^{11} ion cm^{-2} ion dose ("Static" conditions) and the accumulated signal from a 1 to 3×10^{13} ions cm^{-2} dose (Steady State, SS, conditions) using 20 keV Ar_{2000} and $(H_2O)_{6000\text{ or }7000}$ ion beams. The numbers are rounded to reflect 10% measurement uncertainty.

The small arginine molecule, Figure 5a, shows comparatively good signal levels under argon, and under *Static* conditions there is little enhancement of $[M + H]^+$ with the water beam; however, the $[2M + H]^+$ is enhanced by a factor of 14. When signal is accumulated over a dose of 3×10^{13} ions cm^{-2} to *Steady State* as is possible with the J105 instrument, there is a factor of 3 improvement under the water clusters to a very high

DOI: 10.1021/ac504191m
Anal. Chem. 2015, 87, 2367−2374

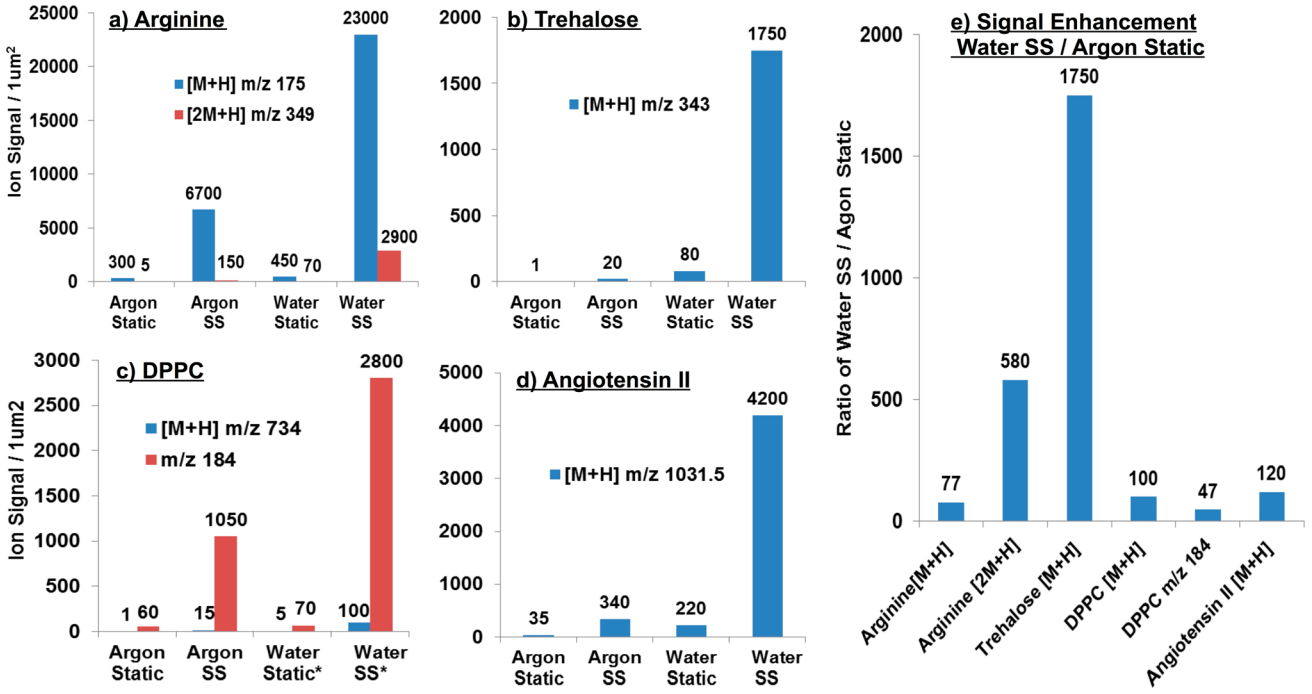

Figure 5. Ion signal/1 μm^2 detected using argon, Ar_{2000}^+, cluster beams and water, $(H_2O)_{7000}^+$, cluster beams using Static conditions, an ion dose of 5 × 10^{11} cm^{-2}, and SS or Steady State conditions, an ion dose of 1.5 to 3 × 10^{13} cm^{-2} for (a) arginine $[M + H]^+$ and $[2M + H]^+$; (b) trehalose $[M + H]^+$; (c) DPPC $[M + H]^+$ and phosphocholine m/z 184 ion; (d) angiotensin II $[M + H]^+$. (e) Ion signal enhancement—ratio of ion signal detected with Water cluster ions under SS conditions compared to Argon cluster ions under Static conditions for Arginine $[M + H]^+$ and $[2M + H]^+$; trehalose $[M + H]^+$; DPPC $[M + H]^+$, and m/z 184 ion; angiotensin II $[M + H]^+$. * refers to $(H_2O)_{4000}$.

signal level per μm^2, and the $[2M + H]^+$ signal is enhanced 19 times. Comparing the $[M + H]^+$ signals detected from trehalose, Figure 5b, using 20 keV Ar_{2000} with those from 20 keV $(H_2O)_{6000\text{ or }7000}$ we see that under *Static* and the accumulated *SS* conditions there is a 80 times increase in signal detection. Although the detected signal for the DPPC, Figure 5c, $[M + H]^+$ ion is enhanced by 15 and 20 times under *Static* and *SS* conditions, the ion yield is still low. Fragmentation of the molecule to form the phosphocholine ion may be a reason. This ion delivers a high signal, which is enhanced little by water clusters under *Static* conditions, although there is a factor 3 enhancement at steady state. The detected signal of this fragment ion will be the consequence of two opposing effects as E/n falls, decreasing neutral phosphocholine fragment formation and increasing protonation activity. The angiotensin II signal levels, Figure 5d, are encouraging showing a 6 and 12 enhancement by water beams in *Static* and *SS* conditions.

This study has been directed toward exploring the ion signal levels that are accessible compared to static analysis by argon cluster beams, when water cluster beams are used in combination with the J105 instrument that is capable of exploiting analysis unconstrained by the static limit such that all the ion signal can be accumulated from 1 μm^2 of analyte. In Figure 5e, the overall signal detection improvement from *Static* conditions under 20 keV Ar_{2000} to accumulated *SS* signal with larger water clusters is shown to vary from 75 times for arginine, through 100 times for DPPC and 120 times for angiotensin II, to 1700 for trehalose. Although there is the inevitable variation with analyte chemistry, the resulting signal levels make submicrometer analysis a great deal more realistic. Upcoming studies will demonstrate this in tissue and cellular imaging. Further increases in yields can be expected with higher energy beams that will enable larger cluster sizes to be accessed in the energy regime around $E/n \sim 3$ eV. On the basis of the observation that doubling the number of cluster components at least doubles the yield, at 40 keV a cluster of 13 000 should give at least double the yields shown in Figure 5. At 60 keV, a cluster beam of 20 000 should at least further double the yield. Of course to fully exploit the benefits of increased ion yield, the spatial resolution of the primary ion beam would be required to be submicrometer with a useable beam current which is a significant technological challenge.

■ ASSOCIATED CONTENT

Supporting Information

Further information on sample preparation, experimental analytical details, and the supplementary figures as detailed in the manuscript. This material is available free of charge via the Internet at http://pubs.acs.org.

■ AUTHOR INFORMATION

Corresponding Author

*E-mail: john.vickerman@manchester.ac.uk.

Notes

The authors declare the following competing financial interest(s): Some financial support for this work came to J.C.V. from Ionoptika Ltd., the supplier of the ion beam system used in the research.

■ ACKNOWLEDGMENTS

This research was funded by the UK Engineering and Physical Sciences Research Council, EPSRC, under Grant EP/K01353X/1. T.K. is grateful to the Fulbright Commission for the provision of a scholarship that enabled him to participate in this research. I.B.R. acknowledges the Mexican Council of

DOI: 10.1021/ac504191m
Anal. Chem. 2015, 87, 2367−2374

Science and Technology, CONACYT, for providing Ph.D. studentship support.

REFERENCES

(1) Vickerman, J. C.; Briggs, D. *TOF-SIMS - Materials Analysis by Mass Spectrometry*; IM Publications and SurfaceSpectra Ltd.: Chichester, U.K., 2013.
(2) Fletcher, J. S.; Vickerman, J. C. *Anal. Chem.* **2013**, *85*, 610−639.
(3) Fornai, L.; Angelini, A.; Kiss, A.; Giskes, F.; Eijkel, G.; Fedrigo, M.; Valente, M. L.; Thiene, G.; Heeren, R. M. A. *Cardiovasc. Res.* **2012**, *93*, S80−S80.
(4) Jungmann, J. H.; Heeren, R. M. A. *J. Proteomics* **2012**, *75*, 5077−5092.
(5) Vickerman, J. C. *Analyst* **2011**, *136*, 2199−2217.
(6) Cheng, J.; Kozole, J.; Hengstebeck, R.; Winograd, N. *J. Am. Soc. Mass. Spectrom.* **2007**, *18*, 406−412.
(7) Delcorte, A. *Appl. Surf. Sci.* **2006**, *252*, 6582−6587.
(8) Fitzgerald, J. J. D.; Kunnath, P.; Walker, A. V. *Anal. Chem.* **2010**, *82*, 4413−4419.
(9) Adriaensen, L.; Vangaever, F.; Gijbels, R. *Anal. Chem.* **2004**, *76*, 6777−6785.
(10) Delcorte, A.; Bertrand, P. *Appl. Surf. Sci.* **2004**, *231*, 250−255.
(11) Restrepo, O.; Prabhakaran, A.; Hamraoui, K.; Wehbe, N.; Yunus, S.; Bertrand, P.; Delcorte, A. *Surf. Interface Anal.* **2010**, *42*, 1030−1034.
(12) Wehbe, N.; Mouhib, T.; Prabhakaran, A.; Bertrand, P.; Delcorte, A. *J. Am. Soc. Mass Spectrom.* **2009**, *20*, 2294−2303.
(13) Davies, N.; Weibel, D. E.; Blenkinsopp, P.; Lockyer, N.; Hill, R.; Vickerman, J. C. *Appl. Surf. Sci.* **2003**, *203*, 223−227.
(14) Touboul, D.; Kollmer, F.; Niehuis, E.; Brunelle, A.; Laprevote, O. *J. Am. Soc. Mass Spectrom.* **2005**, *16*, 1608−1618.
(15) Gillen, G.; Roberson, S. *Rapid Commun. Mass Spectrom.* **1998**, *12*, 1303−1312.
(16) Weibel, D.; Wong, S.; Lockyer, N.; Blenkinsopp, P.; Hill, R.; Vickerman, J. C. *Anal. Chem.* **2003**, *75*, 1754−1764.
(17) Wehbe, N.; Mouhib, T.; Delcorte, A.; Bertrand, P.; Moellers, R.; Niehuis, E.; Houssiau, L. *Anal. Bioanal. Chem.* **2013**, 1−11.
(18) Ichiki, K.; Ninomiya, S.; Nakata, Y.; Honda, Y.; Seki, T.; Aoki, T.; Matsuo, J. *Appl. Surf. Sci.* **2008**, *255*, 1148−1150.
(19) Rabbani, S.; Barber, A. M.; Fletcher, J. S.; Lockyer, N. P.; Vickerman, J. C. *Anal. Chem.* **2011**, *83*, 3793−3800.
(20) Aoyagi, S.; Fletcher, J. S.; Sheraz, S.; Kawashima, T.; Razo, I. B.; Henderson, A.; Lockyer, N. P.; Vickerman, J. C. *Anal. Bioanal. Chem.* **2013**, *405*, 6621−6628.
(21) Kayser, S.; Rading, D.; Moellers, R.; Kollmer, F.; Niehuis, E. *Surf. Interface Anal.* **2013**, *45*, 131−133.
(22) Gnaser, H.; Ichiki, K.; Matsuo, J. *Rapid Commun. Mass Spectrom.* **2012**, *26*, 1−8.
(23) Gnaser, H.; Fujii, M.; Nakagawa, S.; Seki, T.; Aoki, T.; Matsuo, J. *Rapid Commun. Mass Spectrom.* **2013**, *27*, 1490−1496.
(24) Gnaser, H.; Fujii, M.; Nakagawa, S.; Seki, T.; Aoki, T.; Matsuo, J. *Int. J. Mass Spectrom.* **2014**, *360*, 54−57.
(25) Gnaser, H.; Ichiki, K.; Matsuo, J. *Surf. Interface Anal.* **2013**, *45*, 138−142.
(26) Ninomiya, S.; Ichiki, K.; Yamada, H.; Nakata, Y.; Seki, T.; Aoki, T.; Matsuo, J. *Surf. Interface Anal.* **2011**, *43*, 221−224.
(27) Angerer, T. B.; Blenkinsopp, P.; Fletcher, J. S. *Int. J. Mass Spectrom.* **2014**, DOI: 10.1016/j.ijms.2014.05.015.
(28) Seah, M. P.; Havelund, R.; Gilmore, I. S. *J. Phys. Chem. C* **2014**, *118*, 12862−12872.
(29) Delcorte, A.; Garrison, B. J.; Hamraoui, K. *Anal. Chem.* **2009**, *81*, 6676−6686.
(30) Czerwinski, B.; Postawa, Z.; Garrison, B. J.; Delcorte, A. *Nucl. Instrum. Methods Phys. Res, Sect. B* **2013**, *303*, 23−27.
(31) Postawa, Z.; Paruch, R.; Rzeznik, L.; Garrison, B. J. *Surf. Interface Anal.* **2013**, *45*, 35−38.
(32) Roddy, T. P.; Cannon, D. M.; Ostrowski, S. G.; Ewing, A. G.; Winograd, N. *Anal. Chem.* **2003**, *75*, 4087−4094.
(33) Cheng, J.; Winograd, N. *Anal. Chem.* **2005**, *77*, 3651−3659.
(34) Piwowar, A. M.; Lockyer, N. P.; Vickerman, J. C. *Anal. Chem.* **2009**, *81*, 1040−1048.
(35) Conlan, X. A.; Lockyer, N. P.; Vickerman, J. C. *Rapid Commun. Mass Spectrom.* **2006**, *20*, 1327−1334.
(36) Mouhib, T.; Delcorte, A.; Poleunis, C.; Bertrand, P. *J. Am. Soc. Mass. Spectrom.* **2010**, *21*, 2005−2010.
(37) Mouhib, T.; Poleunis, C.; Moellers, R.; Niehuis, E.; Defrance, P.; Bertrand, P.; Delcorte, A. *Surf. Interface Anal.* **2013**, *45*, 163−166.
(38) Sheraz, S.; Barber, A.; Fletcher, J. S.; Lockyer, N. P.; Vickerman, J. C. *Anal. Chem.* **2013**, *85*, 5654−5658.
(39) Hiraoka, K.; Mori, K.; Asakawa, D. *J. Mass Spectrom.* **2006**, *41*, 894−902.
(40) Ninomiya, S.; Chen, L. C.; Suzuki, H.; Sakai, Y.; Hiraoka, K. *Rapid Commun. Mass Spectrom.* **2012**, *26*, 863−869.
(41) Fujiwara, Y.; Saito, N. *Surf. Interface Anal.* **2014**, n/a−n/a.
(42) Fanourgakis, G. S.; Aprà, E.; Xantheas, S. S. *J. Chem. Phys.* **2004**, *121*, 2655−2663.
(43) Fletcher, J. S.; Rabbani, S.; Henderson, A.; Blenkinsopp, P.; Thompson, S. P.; Lockyer, N. P.; Vickerman, J. C. *Anal. Chem.* **2008**, *80*, 9058−9064.
(44) Hill, R.; Blenkinsopp, P.; Thompson, S.; Vickerman, J.; Fletcher, J. S. *Surf. Interface Anal.* **2011**, *43*, 506−509.
(45) Lee, J. L. S.; Ninomiya, S.; Matsuo, J.; Gilmore, I. S.; Seah, M. P.; Shard, A. G. *Anal. Chem.* **2010**, *82*, 98−105.
(46) Shard, A. G.; Ray, S.; Seah, M. P.; Yang, L. *Surf. Interface Anal.* **2011**, *43*, 1240−1250.
(47) Shard, A. G.; Brewer, P. J.; Green, F. M.; Gilmore, I. S. *Surf. Interface Anal.* **2007**, *39*, 294−298.
(48) Shard, A. G.; Foster, R.; Gilmore, I. S.; Lee, J. L. S.; Ray, S.; Yang, L. *Surf. Interface Anal.* **2011**, *43*, 510−513.
(49) Seah, M. P. *J. Phys. Chem. C* **2013**, *117*, 12622−12632.
(50) Paruch, R. J.; Garrison, B. J.; Mlynek, M.; Postawa, Z. *J. Phys. Chem. Lett.* **2014**, 3227−3230.
(51) Murphy, R. C.; Harrison, K. A. *Mass Spectrom. Rev.* **1994**, *13*, 57−75.
(52) Sostarecz, A. G.; Cannon, D. M.; McQuaw, C. M.; Sun, S. X.; Ewing, A. G.; Winograd, N. *Langmuir* **2004**, *20*, 4926−4932.
(53) Puzo, G.; Prome, J.-C. *Org. Mass Spectrom.* **1984**, *19*, 448−451.
(54) Jaskolla, T.; Karas, M. *J. Am. Soc. Mass. Spectrom.* **2011**, *22*, 976−988.
(55) Garrison, B. J. *Surf. Interface Anal.* **2011**, *43*, 134−136.
(56) Willingham, D.; Brenes, D. A.; Winograd, N.; Wucher, A. *Surf. Interface Anal.* **2011**, *43*, 45−48.

DOI: 10.1021/ac504191m
Anal. Chem. 2015, 87, 2367−2374